Sensory capacity: An information theoretical measure of the performance of a sensor

David Hartich,[1] Andre C. Barato,[1,2] and Udo Seifert[1]

[1]*II. Institut für Theoretische Physik, Universität Stuttgart, 70550 Stuttgart, Germany*
[2]*Max Planck Institute for the Physics of Complex Systems, Nöthnizer Straße 38, 01187 Dresden, Germany*

For a general sensory system following an external stochastic signal, we introduce the sensory capacity. This quantity characterizes the performance of a sensor: sensory capacity is maximal if the instantaneous state of the sensor has as much information about a signal as the whole time series of the sensor. We show that adding a memory to the sensor increases the sensory capacity. This increase quantifies the improvement of the sensor with the addition of the memory. Our results are obtained with the framework of stochastic thermodynamics of bipartite systems, which allows for the definition of an efficiency that relates the rate with which the sensor learns about the signal with the energy dissipated by the sensor, which is given by the thermodynamic entropy production. We demonstrate a general trade-off between sensory capacity and efficiency: if the sensory capacity is equal to its maximum 1, then the efficiency must be less than 1/2. As a physical realization of a sensor we consider a two-component cellular network estimating a fluctuating external ligand concentration as signal. This model leads to coupled linear Langevin equations that allow us to obtain explicit analytical results.

I. INTRODUCTION

The relation between information and thermodynamics is a very active topic, as reviewed in Ref. [1]. Prominently, developments in this field lead to a better understanding of fundamental limits related to dissipation in a computer and of cellular information processing. Much of the renewed interest in this relation between information and thermodynamics is associated with the fact that recent experiments with small systems verify fundamental relations such as the Landauer limit for the erasure of a bit [2,3] and the "conversion of information into work" [4–6]. Theoretical advances in the field include second-law inequalities and fluctuation relations containing an informational term [7–29], generalization of thermodynamics to include information reservoirs [30–39], stochastic thermodynamics of bipartite systems [40–46], and the relation between dissipation and information in biological systems [47–59].

A sensor that learns about (or "measures") an external stochastic signal constitutes a fundamental setup within thermodynamics of information processing. In this case energy is dissipated and the sensor obtains information about the external signal, in contrast to Maxwell's demon, which is another fundamental setup, where information is used to extract work.

General results for the thermodynamics of a sensor have been obtained by Still *et al.* [60]. They have shown that an entropy characterizing how much information the sensor obtains about the external signal is bounded by the dissipated heat. Similarly, we have shown that an entropic rate, dubbed learning rate, is bounded by the thermodynamic entropy production in bipartite systems [55], which allowed for the definition of a thermodynamic efficiency for models related to cellular information processing.

In this paper, using bipartite Markov processes we introduce the sensory capacity, an informational efficacy parameter characterizing the performance of a sensor. This quantity is defined as the learning rate divided by the transfer entropy rate, where the latter quantifies how much information the full time series of the sensor has about the signal. Sensory capacity is positive and bounded by 1. The limit 1 is reached if the information contained in the instantaneous state of the sensor equals the information contained in the whole time series of the sensor, which is the maximum information the sensor can have about the signal.

A bare sensor, i.e., a sensor with only one degree of freedom, is compared to a sensor that contains a memory, which is a second degree of freedom. We show that the addition of a memory to a bare sensor can increase the sensory capacity. This increase in sensory capacity quantifies how much of the information contained in the time series of the bare sensor is stored in the instantaneous state of the memory.

Our results are obtained with coupled linear Langevin equations that constitute a simple example of a bipartite system. These linear Langevin equations are derived from a discrete model for a two-component cellular network estimating an external ligand concentration, which is the signal. The two components of the network are receptors that can bind external ligands and internal proteins that play the role of memory [48,53,54,58,61]. This derivation starting with a physical model for a sensor allows us to provide a clear physical interpretation for the parameters showing up in the Langevin equations and for the thermodynamic entropy production.

The relation between sensory capacity and energy dissipation is also discussed. Particularly, as a main result we show that if the sensory capacity is 1, the efficiency relating learning rate and rate of dissipation must be smaller than 1/2. This result is valid for any bipartite process. The specific trade-off between sensory capacity and efficiency for the coupled linear Langevin equations is analyzed in detail.

The paper in organized as follows. In Sec. II we define discrete bipartite processes and the quantities calculated in the paper. Section III contains the derivation of the coupled linear Langevin equations from the microscopic model for a two-component network. The analysis of the Langevin equations is performed in Sec. IV. The general trade-off between sensory capacity and efficiency is derived in Sec. V. We conclude

in Sec. VI. The continuum limit from a master equation to a Langevin equation in bipartite systems is presented in Appendix A. The uncertainty about the signal given the sensor state and the uncertainty given the sensor trajectory are calculated in Appendix B.

II. BIPARTITE MARKOV PROCESSES AND SENSORY CAPACITY

A. Definition of bipartite systems

A state of the signal is denoted by x and a state of the sensor by y. We consider a quite general framework, where the basic assumptions are that the dynamics of the full system composed by the signal and the sensor is Markovian, the dynamics of the signal is not affected by the sensor whereas the dynamics of the sensor is affected by the signal, and the signal alone is also Markovian. For a Markov jump process these assumptions imply the following transition rates from a state (x,y) to a state (x',y'),

$$w_{yy'}^{xx'} \equiv \begin{cases} w^{xx'} & \text{if } x \neq x' \text{ and } y = y', \\ w_{yy'}^{x} & \text{if } x = x' \text{ and } y \neq y', \\ 0 & \text{if } x \neq x' \text{ and } y \neq y'. \end{cases} \quad (1)$$

Such a Markov process, for which the two variables labeling a state cannot both change in a jump, is called bipartite [41]. The rates (1) correspond to a particular case of a bipartite process since $w^{xx'}$ is independent of y. For bipartite systems in a steady state, which is the regime we consider in this paper, the stationary probability of state (x,y) is written as $P(x,y)$. The marginals of this joint probability are defined as $P(x) \equiv \sum_y P(x,y)$ and $P(y) \equiv \sum_x P(x,y)$. The stationary conditional probabilities read $P(x|y) \equiv P(x,y)/P(y)$ and $P(y|x) \equiv P(x,y)/P(x)$.

Key quantities in this paper are the Shannon entropy and mutual information. The Shannon entropy associated with a random variable A is

$$H[A] \equiv -\sum_a \mathcal{P}(A=a) \ln \mathcal{P}(A=a), \quad (2)$$

where a is a specific realization of A and $\mathcal{P}$ denotes a generic probability. The random variables A can be the instantaneous state of the signal x_t or of the sensor y_t. Furthermore, A can be a full time series of the signal $\{x_{t'}\}_{t' \leqslant t}$ or of the sensor $\{y_{t'}\}_{t' \leqslant t}$. In the first case, the sum in a in Eq. (2) is a sum over all possible states. In the second case, this sum corresponds to a functional integration over all possible trajectories. The conditional Shannon entropy of A given another random variable B is

$$H[A|B] \equiv -\sum_{a,b} \mathcal{P}(A=a,B=b) \ln \mathcal{P}(A=a|B=b). \quad (3)$$

The mutual information between A and B reads

$$I[A:B] \equiv H[A] - H[A|B] = H[B] - H[B|A], \quad (4)$$

where the second equality indicates that the mutual information is symmetric in the variables A and B.

B. Learning rate

The learning rate is defined as [55]

$$l_y \equiv \frac{H[x_t|y_t] - H[x_t|y_{t+dt}]}{dt}, \quad (5)$$

where here and in the following in all expressions that involve a dt in the denominator the limit $dt \to 0$ is assumed. The learning rate quantifies the rate at which the sensor acquires information about the instantaneous signal state x_t, i.e., the rate at which the sensor reduces the uncertainty (as characterized by the conditional Shannon entropy) of the signal due to its dynamics [55]. The learning rate can also be written in terms of mutual information

$$l_y = \frac{I[x_t:y_{t+dt}] - I[x_t:y_t]}{dt}, \quad (6)$$

which is the rate at which the y jumps increase the mutual information between the sensor y and the signal x. This form of the learning rate is also known as "information flow" [40,44,45]. Using the relations

$$\begin{aligned} \mathcal{P}(x_{t+dt}=x'|x_t=x) &= w^{xx'} dt & \text{for } x \neq x', \\ \mathcal{P}(y_{t+dt}=y'|x_t=x,y_t=y) &= w_{yy'}^{x} dt & \text{for } y \neq y' \end{aligned} \quad (7)$$

the learning rate (5) becomes

$$l_y = \sum_{x,y,y'} P(x,y) w_{yy'}^{x} \ln \frac{P(x|y')}{P(x|y)}. \quad (8)$$

In the steady state the learning rate is equal to the rate of Shannon entropy reduction of x due to its coupling with y, which is defined as [42]

$$h_x \equiv \frac{H[x_{t+dt}|y_t] - H[x_t|y_t]}{dt}. \quad (9)$$

This conservation law comes from the relation $\frac{d}{dt} H[x|y] \equiv h_x - l_y = 0$ [55], where h_x is the contribution due to the x jumps, i.e.,

$$h_x = \sum_{x,x',y} P(x,y) w^{xx'} \ln \frac{P(x|y)}{P(x'|y)}. \quad (10)$$

Since in the stationary state $H[y_{t+dt}] = H[y_t]$, the learning rate can also be written in the form

$$l_y = h_x = \frac{I[x_t:y_t] - I[x_{t+dt}:y_t]}{dt}. \quad (11)$$

This expression is similar to the one used in Ref. [60], where within a discrete time formalism the term $I[x_{t+dt}:y_t]$ is identified as "predictive power."

C. Sensory capacity and transfer entropy rate

Transfer entropy is an informational quantity that detects causal influence between two random variables [62]. It plays an important role in the relation between information thermodynamics for causal networks [19], bipartite systems [40,42,45], and feedback-driven systems [18]. The transfer entropy rate
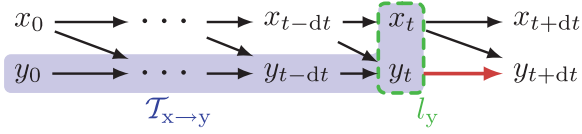
FIG. 1. Learning rate versus transfer entropy rate. The learning rate takes into account only the instantaneous state x_t (dashed green box) to infer the signal x_t, whereas the transfer entropy $\mathcal{T}_{x \to y}$ takes into account the trajectory highlighted by the blue shaded region.

from the signal to the sensor $\mathcal{T}_{x \to y}$ is defined as [42]

$$
\begin{aligned}
\mathcal{T}_{x \to y} &\equiv \frac{H[y_{t+dt}|\{y_{t'}\}_{t' \leqslant t}] - H[y_{t+dt}|\{y_{t'}\}_{t' \leqslant t}, x_t]}{dt} \\
&= \frac{I[y_{t+dt}:x_t|\{y_{t'}\}_{t' \leqslant t}]}{dt} \\
&= \frac{H[x_t|\{y_{t'}\}_{t' \leqslant t}] - H[x_t|y_{t+dt}, \{y_{t'}\}_{t' \leqslant t}]}{dt}.
\end{aligned} \tag{12}
$$

In the third line the similarity to the learning rate (5) is explicit: the transfer entropy rate $\mathcal{T}_{x \to y}$ quantifies how much information the whole sensor trajectory $\{y_{t'}\}_{t' \leqslant t}$ contains about the instantaneous signal x_t, in contrast to the learning rate that considers only the instantaneous state y_t. This difference between the learning rate l_y and the transfer entropy rate $\mathcal{T}_{x \to y}$ is illustrated in Fig. 1. The first line of Eq. (12) contains the standard definition of transfer entropy from the signal to the sensor [62], which can be described as the reduction on the conditional Shannon entropy of y_{t+dt} given $\{y_{t'}\}_{t' \leqslant t}$ by the further knowledge of the signal state x_t.

As shown in Ref. [42] $l_y \leqslant \mathcal{T}_{x \to y}$, which simply means that the whole trajectory of the sensor $\{y_{t'}\}_{t' \leqslant t}$ contains more information about the instantaneous signal x_t than the instantaneous state of the sensor y_t. Based on this inequality we propose the definition

$$
C \equiv \frac{l_y}{\mathcal{T}_{x \to y}} \leqslant 1 \tag{13}
$$

that we call sensory capacity. If $C = 1$ the sensor has reached an information theoretical limit and its instantaneous state has the maximum possible information, which is the information contained in the whole time series of the sensor. On a side note, as a result related to the fact that the full time series of a sensor contains more information about the signal than its instantaneous state, it has been shown that an information-driven machine using the whole history of measurements can extract more work than a machine that only takes the last measurement into account [22,27]. This increase in work extraction is characterized by a gain parameter that, like the sensory capacity, is positive and bounded by 1.

Our sensory capacity that quantifies the performance of a sensor for a specific signal should not be confused with the standard channel capacity in information theory [63]. This second quantity is defined for a different setup of two static random variables, which are the input and the output. For a given conditional probability of the output given the input, the channel capacity is the maximal mutual information between input and output, where the maximization is over the input probability distribution [63].

D. Thermodynamic entropy production and efficiency

The thermodynamic entropy production [64] for bipartite processes has two contributions. One is due to jumps that change the state of the signal,

$$
\sigma_x \equiv \sum_{x,x'} P(x) w^{xx'} \ln \frac{w^{xx'}}{w^{x'x}}. \tag{14}
$$

If the bare signal is an equilibrium process, which is the case for the examples considered in this paper, $\sigma_x = 0$. The second contribution arises from jumps that change the state of the sensor, which reads

$$
\sigma_y \equiv \sum_{x,y,y'} P(x,y) w^x_{yy'} \ln \frac{w^x_{yy'}}{w^x_{y'y}}. \tag{15}
$$

The inequality $l_y \leqslant \sigma_y$ leads to the efficiency [55]

$$
\eta \equiv \frac{l_y}{\sigma_y} \leqslant 1. \tag{16}
$$

This efficiency relates the rate at which the sensor learns about the signal with the rate of free energy dissipation, which is quantified by the thermodynamic entropy production. For the model system in Sec. III, the entropy production has two terms. One is related to work delivered by the external signal and another to free energy dissipation inside the cell.

E. Upper bound on the transfer entropy, coarse-grained entropy production, and coarse-grained learning rate

We now recall the definition of further quantities that will be calculated in this paper. The first quantity is an upper bound on the transfer entropy rate

$$
\overline{\mathcal{T}}_{x \to y} \equiv \frac{H[y_{t+dt}|y_t] - H[y_{t+dt}|y_t, x_t]}{dt} \geqslant \mathcal{T}_{x \to y}. \tag{17}
$$

An important property of this upper bound is that, unlike the transfer entropy rate, it can be written in terms of the stationary distribution as [42]

$$
\overline{\mathcal{T}}_{x \to y} = \sum_{x,y,y'} P(x,y) w^x_{yy'} \ln \frac{w^x_{yy'}}{\overline{w}_{yy'}}, \tag{18}
$$

where

$$
\overline{w}_{yy'} \equiv \sum_x P(x|y) w^x_{yy'}. \tag{19}
$$

The inequality $\overline{\mathcal{T}}_{x \to y} \geqslant \mathcal{T}_{x \to y}$ is obtained by comparing Eq. (12) with Eq. (17), and using relations $H[y_{t+dt}|y_t] \geqslant H[y_{t+dt}|\{y_{t'}\}_{t' \leqslant t}]$ and $H[y_{t+dt}|\{y_{t'}\}_{t' \leqslant t}, x_t] = H[y_{t+dt}|y_t, x_t]$.

The coarse-grained entropy production is obtained by integrating the variable x out, leading to the expression [65]

$$
\tilde{\sigma}_y \equiv \sum_{yy'} P(y) \overline{w}_{yy'} \ln \frac{\overline{w}_{yy'}}{\overline{w}_{y'y}} \geqslant 0. \tag{20}
$$

This $\tilde{\sigma}_y$ is a lower bound on the real entropy production, i.e., $\sigma_y \geqslant \tilde{\sigma}_y$ [65].
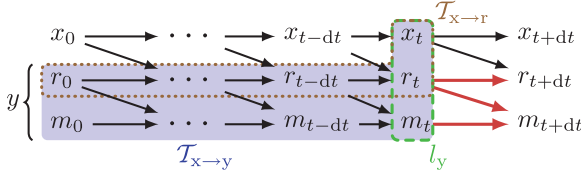
FIG. 2. Illustration of the causal relation $x \to r \to m$ for a sensor $y = (r,m)$ composed of the first layer r and the memory m.

F. Sensor with a memory

We now consider a sensor with two degrees of freedom $y \equiv (r,m)$. We assume that r is the first degree of freedom directly sensing the signal x and m is a memory storing the information collected by r (see [58] for a similar setup). The coarse-grained learning rate is defined as [55]

$$l_r \equiv \frac{H[x_t|r_t] - H[x_t|r_{t+dt}]}{dt}$$

$$= \sum_{x,r,r',m} P(x,r,m) w^x_{(r,m)(r',m)} \ln \frac{P(x|r')}{P(x|r)}, \quad (21)$$

where $w^x_{(r,m)(r',m)}$ denotes the transition rate from (x,r,m) to (x,r',m). The rate at which r alone learns about the signal x is quantified by $l_r \leqslant l_y$ [55]. The transition rates then have the form

$$w^{xx'}_{yy'} \equiv \begin{cases} w^{xx'} & \text{if } x \neq x' \text{ and } y = y', \\ w^x_{rr'} & \text{if } x = x', r \neq r', \text{ and } m = m', \\ w_{(r,m)(r,m')} & \text{if } x = x', r = r', \text{ and } m \neq m', \\ 0 & \text{otherwise}, \end{cases} \quad (22)$$

where $y' = (r',m')$. The transition rates (22) imply the causal relation $x \to r \to m$, which is illustrated in Fig. 2. Therefore, the coarse-grained learning rate in Eq. (21) becomes

$$l_r = \sum_{x,r,r'} P(x,r) w^x_{rr'} \ln \frac{P(x|r')}{P(x|r)}. \quad (23)$$

Transition rates with three variables that do not change simultaneously in a jump, as in Eq. (22), form a tripartite system, which is a particular case of a multipartite Markov process [46]. The transfer entropy in this case fulfills the relation

$$\mathcal{T}_{x \to y} = \mathcal{T}_{x \to r}, \quad (24)$$

where

$$\mathcal{T}_{x \to r} \equiv \frac{H[r_{t+dt}|\{r_{t'}\}_{t' \leqslant t}] - H[r_{t+dt}|\{r_{t'}\}_{t' \leqslant t}, x_t]}{dt}. \quad (25)$$

Relation (24) means that the transfer entropy from the signal x to the sensor $y = (r,m)$ is equal to the transfer entropy from x to the first layer of the sensor r. This relation is a consequence of the causal relation $x \to r \to m$ and can be demonstrated as follows.

By defining $z_t \equiv (x_t,r_t,m_t)$ the conditional probability $\mathcal{P}(z_{t+dt}|z_t)$ can be written as

$$\mathcal{P}(z_{t+dt}|z_t) = \mathcal{P}(x_{t+dt}|x_t)\mathcal{P}(r_{t+dt}|x_t,r_t)\mathcal{P}(m_{t+dt}|r_t,m_t), \quad (26)$$

which follows from the structure of the rates in Eq. (22). From the definition of the conditional Shannon entropy (3), Eq. (26)

implies the following relations:

$$H[z_{t+dt}|z_t]$$
$$= H[x_{t+dt}|x_t] + H[r_{t+dt}|x_t,r_t] + H[m_{t+dt}|r_t,m_t] \quad (27)$$

and

$$H[y_{t+dt}|y_t,x_t] \equiv H[r_{t+dt},m_{t+dt}|r_t,m_t,x_t]$$
$$= H[r_{t+dt}|r_t,x_t] + H[m_{t+dt}|r_t,m_t]. \quad (28)$$

For large time t, the Markov property $\mathcal{P}(z_{t+dt}|z_t) = \mathcal{P}(z_{t+dt}|\{z_{t'}\}_{t' \leqslant t})$ and (26) lead to

$$H[y_{t+dt}|\{y_{t'}\}_{t' \leqslant t}] = H[r_{t+dt},m_{t+dt}|\{r_{t'}\}_{t' \leqslant t},\{m_{t'}\}_{t' \leqslant t}]$$
$$= H[r_{t+dt}|\{r_{t'}\}_{t' \leqslant t}] + H[m_{t+dt}|m_t,r_t]. \quad (29)$$

Finally, from Eqs. (28) and (29) we obtain the transfer entropy rate (12) in the form

$$\mathcal{T}_{x \to y} = \frac{H[y_{t+dt}|\{y_{t'}\}_{t' \leqslant t}] - H[y_{t+dt}|y_t,x_t]}{dt}$$
$$= \frac{H[r_{t+dt}|\{r_{t'}\}_{t' \leqslant t}] - H[r_{t+dt}|r_t,x_t]}{dt}, \quad (30)$$

which after a comparison with (25) yields the desired equality (24).

From the definition of the upper bound on the transfer entropy rate (17) and Eq. (26) we obtain

$$\overline{\mathcal{T}}_{x \to y} = \frac{H[r_{t+dt}|r_t,m_t] - H[r_{t+dt}|r_t,x_t]}{dt}. \quad (31)$$

Hence, the inequality $H[r_{t+dt}|r_t,m_t] \leqslant H[r_{t+dt}|r_t]$ leads to

$$\overline{\mathcal{T}}_{x \to y} \leqslant \overline{\mathcal{T}}_{x \to r}, \quad (32)$$

where

$$\overline{\mathcal{T}}_{x \to r} \equiv \frac{H[r_{t+dt}|r_t] - H[r_{t+dt}|r_t,x_t]}{dt}. \quad (33)$$

Note that inequality (32) is the opposite to what happens to the learning rate, i.e., $l_r \leqslant l_y$. The chain of inequalities that summarizes the inequalities discussed in this section involving learning rate, coarse-grained learning rate, transfer entropy rates, and upper bounds on transfer entropy rates is given by

$$l_r \leqslant l_y \leqslant \mathcal{T}_{x \to r} = \mathcal{T}_{x \to y} \leqslant \overline{\mathcal{T}}_{x \to y} \leqslant \overline{\mathcal{T}}_{x \to r}. \quad (34)$$

The adaptation of the expressions from this section to the continuous limit, where the master equation becomes a Fokker-Planck equation, is presented in Appendix A.

III. CELLULAR TWO-COMPONENT NETWORK SENSING AN EXTERNAL LIGAND CONCENTRATION

As a physical realization of a sensor we consider the cellular two-component network sensing a fluctuating ligand concentration shown in Fig. 3 (see [58] for a similar setup). The signal x is related to the external ligand concentration s through the expression $x = \ln(s/s_0)$, where s_0 is some base concentration value. The first layer of the two-component network, which is the degree of freedom directly sensing the external concentration, is composed by the receptors. Each receptor can be either bound by a ligand or empty, with the
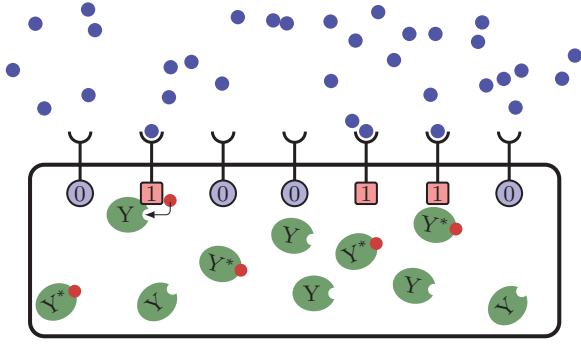
FIG. 3. Cellular two-competent network sensing an external ligand concentration. The total number of receptors is $N_b = 7$ and the number of occupied receptors is $n_b = 3$. The number of internal proteins, which constitute the memory, is $N_y = 10$ with $n_y = 4$ of them phosphorylated. The number of occupied receptors affects the transition rates related to the phosphorylation of internal proteins.

possible values of the number of bound receptors given by $n_b = 0, 1, \ldots, N_b$, where N_b is the total number of receptors. The second layer of the two-component network is composed by internal proteins Y that can be phosphorylated to the state Y^*. The number of proteins in this phosphorylated form takes the values $n_y = 0, 1, \ldots, N_y$, where N_y is the total number of proteins. This second degree of freedom is the memory of the sensor: the phosphorylation/dephosphorylation reaction rates depend on n_b, whereas n_y has no influence on the transition rates changing the number of occupied receptors. A state of the sensor is fully characterized by $y = (n_b, n_y)$.

The rates with which the concentration changes are written as

$$w_{\pm}^{(1)}(x) = \frac{D_x}{dx^2} \exp\left(\mp \frac{\omega_x x}{2 D_x} dx\right), \quad (35)$$

where x is a multiple of dx and the "+" sign indicates a jump from x to $x + dx$ while the "−" sign indicates a jump from x to $x - dx$. As shown in Appendix A, the limit $dx \to 0$ yields the continuous Langevin equation

$$\dot{x}_t = -\omega_x x_t + \xi_t^x, \quad (36)$$

for the dynamics of the signal. The white noise ξ_t^x fulfills the relation

$$\left\langle \xi_t^x \xi_{t'}^x \right\rangle = 2 D_x \delta(t - t'), \quad (37)$$

where the brackets denote an average over stochastic trajectories.

The number of occupied receptors changes with rates

$$w_{+}^{(2)}(x, n_b) = \omega_r^+(x)[N_b - n_b],$$
$$w_{-}^{(2)}(x, n_b) = \omega_r^-(x) n_b, \quad (38)$$

where $\omega_r^+(x)$ is the rate for the binding of a ligand to any free receptor and $\omega_r^-(x)$ is the rate for the unbinding of a ligand from any occupied receptor. These rates fulfill the generalized detailed balance relation $\omega_r^+(x)/\omega_r^-(x) = \exp[\Delta F(x)]$, where $\Delta F(x)$ is the free energy difference between empty and occupied receptor and $k_B T \equiv 1$ throughout. It is assumed that the number of ligands is so large that binding and unbinding events do not alter the external ligand concentration.

The phosphorylation reaction of a single internal protein takes place with rates

$$Y + ATP \underset{n_b \kappa_-}{\overset{n_b \kappa_+}{\rightleftharpoons}} Y^* + ADP, \quad (39)$$

which are proportional to the number of bound receptors n_b. Besides this chemical reaction the internal proteins can also be dephosphorylated through the reaction

$$Y^* \underset{\nu_-}{\overset{\nu_+}{\rightleftharpoons}} Y + P_i, \quad (40)$$

where the rates are independent of n_b. The rates in Eqs. (39) and (40) fulfill the relation $\ln[\kappa_+ \nu_+ / (\kappa_- \nu_-)] \equiv \Delta \mu$, where $\Delta \mu \equiv \mu_{ATP} - \mu_{ADP} - \mu_{P_i}$ is the free energy liberated in one ATP hydrolysis. We define the total transition rates for individual proteins as

$$\omega_m^+(n_b) \equiv n_b \kappa_+ + \nu_-,$$
$$\omega_m^-(n_b) \equiv n_b \kappa_- + \nu_+. \quad (41)$$

With these rates for the change of an individual protein we obtain the transition rates for a change in the variable n_y,

$$w_{+}^{(3)}(n_b, n_y) = \omega_m^+(n_b)[N_y - n_y],$$
$$w_{-}^{(3)}(n_b, n_y) = \omega_m^-(n_b) n_y. \quad (42)$$

The entropy production due to the sensor jumps σ_y has two contributions. The first is due to jumps that change the receptors occupancy

$$\sigma_r = \sum_{x, n_b} J_r(x, n_b) \ln \frac{w_{+}^{(2)}(x, n_b)}{w_{-}^{(2)}(x, n_b + 1)}, \quad (43)$$

where

$$J_r(x, n_b)$$
$$\equiv P(x, n_b) w_{+}^{(2)}(x, n_b) - P(x, n_b + 1) w_{-}^{(2)}(x, n_b + 1) \quad (44)$$

is the probability current. The second is due to jumps that change the number of phosphorylated internal proteins

$$\sigma_m = \sum_{n_b, n_y} J_m(n_b, n_y) \ln \frac{w_{+}^{(3)}(n_b, n_y)}{w_{-}^{(3)}(n_b, n_y + 1)}, \quad (45)$$

where

$$J_m(n_b, n_y) \equiv P(n_b, n_y) w_{+}^{(3)}(n_b, n_y)$$
$$- P(n_b, n_y + 1) w_{-}^{(3)}(n_b, n_y + 1). \quad (46)$$

The quantity σ_r corresponds to the rate of dissipated heat due to binding and unbinding of ligands at different concentrations values. This dissipated heat is compensated by work that is done by the external signal. The quantity σ_y is the rate of dissipated free energy related to the consumption of ATP inside the cell. Actually, since we are not considering each individual link with the phosphorylation and dephosphorylation chemical reactions, but rather the total transition rates in Eq. (41), σ_m is a lower bound on the rate of heat dissipated due to ATP consumption. A thorough discussion on the physical origin of different terms in the entropy production for related models can be found in Ref. [55].

As shown in Appendix A, taking the linear noise approximation and assuming a signal with small fluctuations, the transition rates in Eqs. (35), (38), and (42) lead to the Langevin equations

$$
\begin{aligned}
\dot{x}_t &= -\omega_{\mathrm{x}} x_t + \xi_t^{\mathrm{x}} && \text{(signal)}, \\
\dot{r}_t &= -\omega_{\mathrm{r}}(r_t - x_t) + \xi_t^{\mathrm{r}} && \text{(sensor)}, \\
\dot{m}_t &= -\omega_{\mathrm{m}}(m_t - r_t) + \xi_t^{\mathrm{m}} && \text{(memory)},
\end{aligned}
\tag{47}
$$

where $\langle \xi_t^i \xi_{t'}^j \rangle = 2D_i \delta_{ij} \delta(t - t')$ for $i,j = \mathrm{x,r,m}$. The variable r is related to the number of bound receptors, as shown in Eq. (A17), and the memory m to the number of phosphorylated internal proteins, as shown in Eq. (A18). The precise relations between the parameters in these equations and the transition rates can be found in Eqs. (A13) and (A20). There are three key points about these relations. First, for $\Delta\mu = 0$, i.e., without free energy dissipation due to ATP hydrolysis inside the cell, the memory becomes decoupled from the receptor and has no information about the signal, which in Eq. (47) implies $D_{\mathrm{m}} \to \infty$. Second, the noise amplitude D_{r} is inversely proportional to the total number of receptors N_{b}. Third, the noise amplitude D_{m} is inversely proportional to the total number of internal proteins N_{y}.

IV. SENSORY CAPACITY AND EFFICIENCY FOR MODEL SYSTEM

A. Bare sensor

First we consider a bare sensor without memory, i.e., the Langevin equations (47) without the variable m. We use the subscript r for the sensory capacity C_{r} and the efficiency η_{r} for the bare sensor of this subsection in order to differentiate it from the sensor with a memory analyzed in the next subsection. The corresponding Lyapunov equation for the covariance matrix

$$
\boldsymbol{\Sigma} = \begin{pmatrix} \Sigma_{\mathrm{xx}} & \Sigma_{\mathrm{xr}} \\ \Sigma_{\mathrm{rx}} & \Sigma_{\mathrm{rr}} \end{pmatrix} \equiv \begin{pmatrix} \langle x_t x_t \rangle & \langle x_t r_t \rangle \\ \langle r_t x_t \rangle & \langle r_t r_t \rangle \end{pmatrix}
\tag{48}
$$

reads [66,67]

$$
\dot{\boldsymbol{\Sigma}} = -\mathbf{A}\boldsymbol{\Sigma} - \boldsymbol{\Sigma}\mathbf{A}^\top + 2\mathbf{D},
\tag{49}
$$

where

$$
\mathbf{A} \equiv \begin{pmatrix} \omega_{\mathrm{x}} & 0 \\ -\omega_{\mathrm{r}} & \omega_{\mathrm{r}} \end{pmatrix} \quad \text{and} \quad \mathbf{D} \equiv \begin{pmatrix} D_{\mathrm{x}} & 0 \\ 0 & D_{\mathrm{r}} \end{pmatrix}.
\tag{50}
$$

The steady state solution of (49) is

$$
\boldsymbol{\Sigma} = \mathcal{E}_{\mathrm{x}}^2 \begin{pmatrix} 1 & \frac{\nu_{\mathrm{r}}}{\nu_{\mathrm{r}}+1} \\ \frac{\nu_{\mathrm{r}}}{\nu_{\mathrm{r}}+1} & \left[\frac{\nu_{\mathrm{r}}}{\nu_{\mathrm{r}}+1} + \frac{B_{\mathrm{r}}}{\nu_{\mathrm{r}}}\right] \end{pmatrix},
\tag{51}
$$

where $\mathcal{E}_{\mathrm{x}}^2 \equiv D_{\mathrm{x}}/\omega_{\mathrm{x}}$ is the signal variance, $\nu_{\mathrm{r}} \equiv \omega_{\mathrm{r}}/\omega_{\mathrm{x}}$, and $B_{\mathrm{r}} \equiv D_{\mathrm{r}}/D_{\mathrm{x}}$.

As shown in Appendix A, the learning rate is

$$
l_{\mathrm{r}} = \omega_{\mathrm{x}} \left[\frac{\nu_{\mathrm{r}}^3}{\nu_{\mathrm{r}}^2 + B_{\mathrm{r}}(1 + \nu_{\mathrm{r}})^2} \right].
\tag{52}
$$
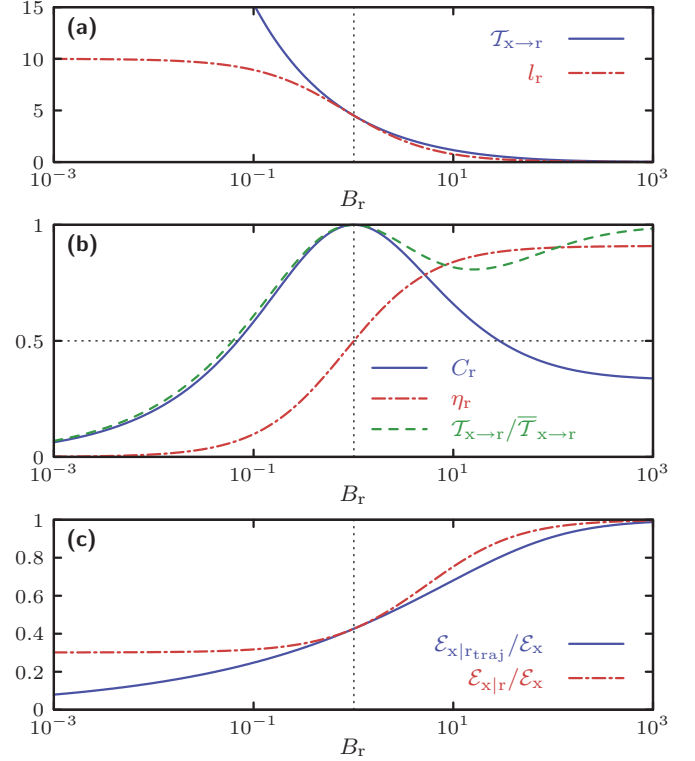
FIG. 4. Sensor performance as a function of sensor noise $B_{\mathrm{r}} = D_{\mathrm{r}}/D_{\mathrm{x}}$. (a) Transfer entropy $\mathcal{T}_{\mathrm{x}\to\mathrm{r}}$ and learning rate l_{r} are displayed. The vertical dotted line at $B_{\mathrm{r}} = \nu_{\mathrm{r}}^2/(\nu_{\mathrm{r}}^2 - 1)$ indicates the value for which $C_{\mathrm{r}} = 1$, i.e., $l_{\mathrm{r}} = \mathcal{T}_{\mathrm{x}\to\mathrm{r}}$. (b) Efficiency ($\eta_{\mathrm{r}} = l_{\mathrm{r}}/\sigma_{\mathrm{r}}$) and capacity ($C_{\mathrm{r}} = l_{\mathrm{r}}/\mathcal{T}_{\mathrm{x}\to\mathrm{r}}$) of the bare sensor. At maximal capacity $C_{\mathrm{r}} = 1$ the efficiency is $\eta_{\mathrm{r}} = 1/2$ and $\mathcal{T}_{\mathrm{x}\to\mathrm{r}} = \overline{\mathcal{T}}_{\mathrm{x}\to\mathrm{r}}$. (c) Comparison of errors. For $C_{\mathrm{r}} = 1$ the inequality $\mathcal{E}_{\mathrm{x}|\mathrm{r_{traj}}} \leqslant \mathcal{E}_{\mathrm{x}|\mathrm{r}}$ saturates. Parameters: $\omega_{\mathrm{x}} \equiv 1, D_{\mathrm{x}} \equiv 0.1, \nu_{\mathrm{r}} = \omega_{\mathrm{r}}/\omega_{\mathrm{x}} \equiv 10$.

The transfer entropy rate for the linear Langevin equations (47) is given by [45]

$$
\mathcal{T}_{\mathrm{x}\to\mathrm{r}} = \frac{\omega_{\mathrm{x}}}{2}\left(\sqrt{1 + \frac{\nu_{\mathrm{r}}^2}{B_{\mathrm{r}}}} - 1 \right).
\tag{53}
$$

The learning rate and transfer entropy rate as functions of B_{r} are plotted in Fig. 4(a). Both quantities get smaller as the noise amplitude of the sensor gets larger. At an intermediate value of $B_{\mathrm{r}} = \nu_{\mathrm{r}}^2/(\nu_{\mathrm{r}}^2 - 1)$ learning rate and transfer entropy become the same leading to a sensory capacity $C_{\mathrm{r}} = 1$, as shown in Fig. 4(b).

Since the bare sensor does not have a memory there is no ATP consumption inside the cell and the entropy production is equal to the rate of work delivered by the external signal, which, as calculated in Appendix A in Eq. (A39), is

$$
\sigma_{\mathrm{r}} = \omega_{\mathrm{x}} \frac{\nu_{\mathrm{r}}^2}{B_{\mathrm{r}}(1 + \nu_{\mathrm{r}})}.
\tag{54}
$$

This entropy production decreases with B_{r}; i.e., a sensor with smaller noise amplitude, which can be obtained by increasing the number of receptors [see Eq. (A14)], implies more energy dissipation. In Fig. 4(b) the thermodynamic efficiency is compared with sensory capacity. The efficiency increases with

B_r. For $B_r = v_r^2/(v_r^2 - 1)$, where $C_r = 1$, the efficiency is $\eta_r = 1/2$. As we show in Sec. V there is a general trade-off between efficiency and sensory capacity, with $C = 1$ implying $\eta \leqslant 1/2$.

The upper bound on the transfer entropy rate, calculated in Appendix A, reads

$$\overline{\mathcal{T}}_{x \to r} = \frac{\omega_x v_r^2}{4 B_r}\left[1 - \frac{v_r^3}{v_r^3 + v_r^2 + B_r(1 + v_r)^2}\right]. \quad (55)$$

This quantity has also been calculated in Ref. [59]. Comparing the upper bound with the transfer entropy rate in Fig. 4(b) we observe that for this model when sensory capacity is 1 we have $l_r = \mathcal{T}_{x \to r} = \overline{\mathcal{T}}_{x \to r}$. This fact plays an important role in the general trade-off between sensory capacity and efficiency proved in Sec. V.

In Appendix B we define the uncertainties $\mathcal{E}_{x|r}$ and $\mathcal{E}_{x|r_{traj}}$ about the signal given the sensor state and the sensor trajectory, respectively. As shown in Appendix B, $\mathcal{E}_{x|r_{traj}}^2$ is proportional to the transfer entropy rate $\mathcal{T}_{x \to r}$ and $\mathcal{E}_{x|r}^2$ is proportional to the upper bound $\overline{\mathcal{T}}_{x \to r}$ for the present model. Hence, the equality between transfer entropy rate and upper bound for $C_r = 1$ implies that both uncertainties are also the same, as shown in Fig. 4(c).

B. Memory increases sensory capacity

For the regimes where the bare sensor does not reach a sensory capacity close to 1, it is possible to increase this sensory capacity by adding a memory to the bare sensor, which leads to the third equation in Eq. (47). The Lyapunov equation (49) for this case has the 3×3 matrices

$$\mathbf{A} = \begin{pmatrix} \omega_x & 0 & 0 \\ -\omega_r & \omega_r & 0 \\ 0 & -\omega_m & \omega_m \end{pmatrix} \quad \text{and} \quad \mathbf{D} \equiv \begin{pmatrix} D_x & 0 & 0 \\ 0 & D_r & 0 \\ 0 & 0 & D_m \end{pmatrix}. \quad (56)$$

The stationary solution of (49) is too long to be displayed here.

The expression for the learning rate l_y is given in Appendix A in Eq. (A45). As shown in Eq. (24), the addition of the memory does not change the transfer entropy $\mathcal{T}_{x \to y} = \mathcal{T}_{x \to r}$ which remains as given by (53). The coarse-grained learning rate l_r is the learning rate for the bare sensor calculated in Eq. (52). The quantities l_y, l_r, and $\mathcal{T}_{x \to r}$ are plotted in Fig. 5(a) as a function of the noise amplitude $B_m \equiv D_m/D_x$. For larger values of B_m the learning rate l_y becomes equal to l_r, and the learning rate does now increase substantially with the addition of a memory with small noise amplitude. By decreasing the noise amplitude l_y increases until it reaches the transfer entropy $\mathcal{T}_{x \to r}$ for small B_m. Hence, the sensory capacity C increases with decreasing B_m, as shown in Fig. 5(b).

The rate of free energy dissipation has now two contributions, i.e., $\sigma_y = \sigma_r + \sigma_m$. The σ_r given by (54) corresponds to the work done by the external signal. The additional term, which is derived in Appendix A in Eq. (A40), is given by

$$\sigma_m = \omega_x \frac{v_m^2\big[v_r^2 + B_r(1 + v_m)(1 + v_r)\big]}{B_m(1 + v_m)(1 + v_r)(v_m + v_r)}, \quad (57)$$

where $v_m \equiv \omega_m/\omega_x$. This σ_m is a lower bound on the rate of dissipated free energy due to ATP consumption. From
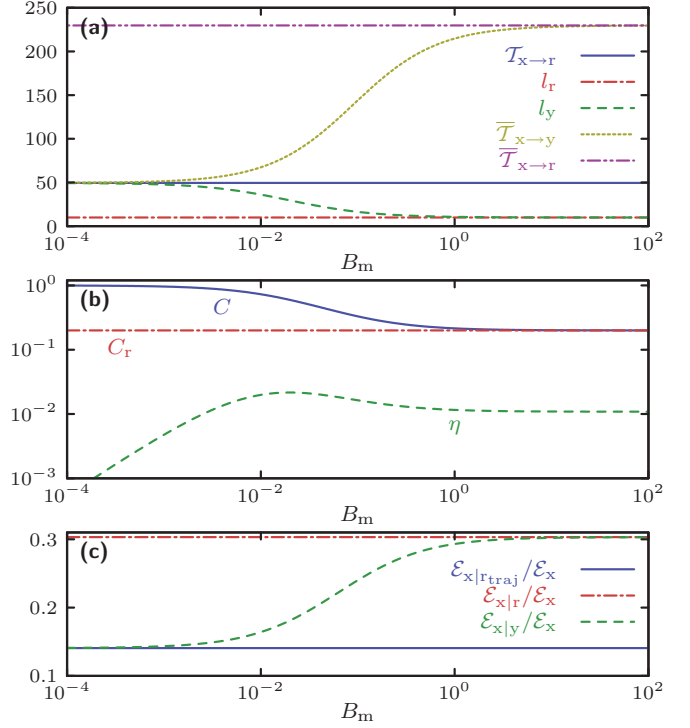

FIG. 5. Effect of a memory. (a) Transfer entropy $\mathcal{T}_{x \to r}$, learning rate of the bare sensor l_r and of the full sensor l_y (including the memory) as a function of the memory noise $B_m = D_m/D_x$. The transfer entropy estimate $\overline{\mathcal{T}}_{x \to y}$ and the learning rate l_y approach $\mathcal{T}_{x \to r}$ for $B_m \to 0$. (b) Sensory capacities $C = l_y/\mathcal{T}_{x \to r}$ and $C_r = l_r/\mathcal{T}_{x \to r}$ in comparison with thermodynamical efficiency $\eta = l_y/\sigma_y$. (c) Effect of memory on error. The error $\mathcal{E}_{x|y}$ corresponding to the full sensor state approaches the minimal error $\mathcal{E}_{x|r_{traj}}$ for $B_m \to 0$. Parameters: $\omega_x \equiv 1$, $D_x \equiv 10^{-1}$, $v_r \equiv \omega_r/\omega_x \equiv 10$, $B_r = D_r/D_x \equiv 10^{-2}$, and $v_m \equiv \omega_m/\omega_x \equiv \sqrt{1 + v_r^2/B_r} \simeq 100$.

expression (57), the decrease in the noise amplitude D_m, which leads to an increase in sensory capacity, implies an increase in the rate of ATP consumption inside the cell. Adding a dissipative memory to a bare sensor can lead to an increase in sensory capacity. This increase corresponds to how much of the information about the trajectory $\{r_{t'}\}_{t' \leqslant t}$ is contained in the instantaneous state of the memory m_t.

For fixed B_m, the sensory capacity C as a function of $v_m \equiv \omega_m/\omega_x$ has a maximum, as shown in the contour plot in Fig. 6. Therefore, for a given ω_x, which characterizes the time scale of changes in the external signal, the memory has an optimal ω_m, which characterizes the time scale of changes in the memory. A sensory capacity close to 1 is reached for small B_m and $v_m \approx \sqrt{1 + v_r^2/B_r}$, as indicated by the red region in Fig. 6.

A larger σ_m leads to a lower efficiency, as shown in Fig. 5(b). Adding a memory with a high rate of dissipation due to ATP consumption can increase a low sensory capacity to the limit $C = 1$. In this case when $C = 1$ the efficiency is small due to the high dissipation of the memory. For example, the maximal efficiency that is achieved in the region plotted in Fig. 6 is $\eta \simeq 0.024$. In this regime of high internal dissipation the efficiency does not seem to be a relevant quantity to characterize the performance of the sensor, which is rather given by sensory capacity.
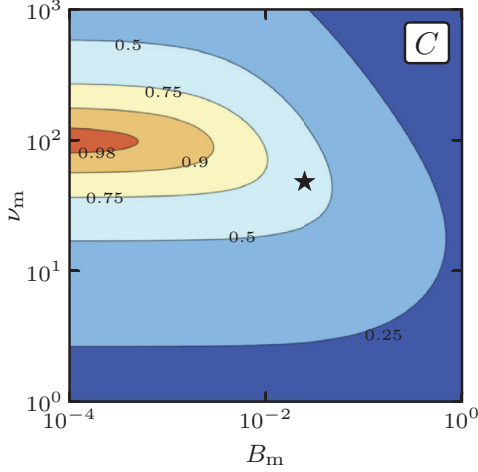
FIG. 6. Effect of memory parameters ν_m and B_m on the sensory capacity. For $\nu_m = \sqrt{1 + \nu_r^2 / B_r} \simeq 10^2$ and $B_m \to 0$ the capacity saturates ($C \to 1$). The star ($\bigstar$) marks the parameter $(\nu_m^\star, B_m^\star)$ for which the efficiency η is maximal (here $\eta^\star \simeq 0.024$). The remaining parameters are chosen as in Fig. 5.

As shown in Appendix B, for a sensor with a memory, the uncertainty taking the instantaneous state of the sensor into account is proportional to the upper bound on the transfer entropy rate. As is the case of the transfer entropy, the uncertainty taking the full time series of the sensor into account does not change with the addition of the memory. Therefore, also for the present case $C = 1$ implies that both uncertainties are equal, as shown in Fig 5(c).

V. TRADE-OFF BETWEEN SENSORY CAPACITY AND EFFICIENCY

A. Trade-off for model system

There are two situations for which the maximal sensory capacity $C = 1$ can be reached. Either the parameters related to the signal and the first layer of the sensor are chosen in such a way that there is no further information in the trajectory $\{r_{t'}\}_{t' \leqslant t}$ as compared to the instantaneous state r_t or a dissipative memory is added to the sensor. In the first case, the efficiency is $\eta = 1/2$ for $C = 1$ and in the other case $\eta < 1/2$ due to the extra dissipation inside the cell.

The trade-off between sensory capacity and efficiency for the model system in Eq. (47) is shown in Fig. 7. For the bare sensor we obtain the bounds

$$4\eta_r(1 - \eta_r) \leqslant C_r \leqslant 2\sqrt{\eta_r(1 - \eta_r)}, \qquad (58)$$

which are derived in the following way. From (52) and (54) the efficiency reads

$$\eta_r = \frac{l_r}{\sigma_r} = \frac{B_r \nu_r (1 + \nu_r)}{\nu_r^2 + B_r (1 + \nu_r)^2}, \qquad (59)$$

and from (52) and (53) the sensory capacity reads

$$C_r = \frac{l_r}{\mathcal{T}_{x \to r}} = \frac{2\nu_r^3}{\left[\nu_r^2 + B_r(1 + \nu_r^2)\right]\left[\sqrt{1 + \nu_r^2/B_r} - 1\right]}. \qquad (60)$$
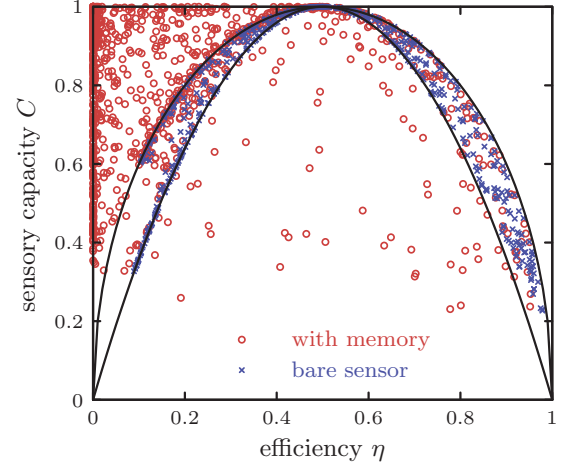

FIG. 7. Trade-off between capacity C and efficiency η. The parameters for the bare sensor ν_r and B_r are chosen at random with $10^{-1} \leqslant \nu_r, B_r \leqslant 10^2$. For the sensor with memory, in addition, the parameters ν_m and B_m are chosen in the same way. The solid lines indicate the bounds $4\eta(1 - \eta) \leqslant C \leqslant 2\sqrt{\eta(1 - \eta)}$ for the bare sensor. Our numerics indicates that the upper bound $C \leqslant 2\sqrt{\eta(1 - \eta)}$ is also valid for the sensor with memory for $\eta \geqslant 1/2$.

The upper (lower) bound in Eq. (58) is obtained by maximizing (minimizing) the capacity (60) with respect to the variables $\nu_r, B_r \geqslant 0$ with the constraint that (59) is fixed. Most prominently, the scatter plot in Fig. 7 shows that the upper bound in Eq. (58) also applies for the full sensor with a memory in the region $\eta \geqslant 1/2$.

B. General proof

We now prove a general trade-off between sensory capacity and efficiency: a sensory capacity $C = 1$ implies $\eta \leqslant 1/2$. Our proof depends on the reasonable assumption that for any sensor it is possible to create a fictitious memory such that the instantaneous state of the fictitious sensor, composed of the sensor and the fictitious memory, contains the whole history of the sensor. From the calculations for the model system in Sec. IV, we expect this fictitious memory to have two general characteristics. First, it must be precise. For the model system this precision is characterized by a small D_m in Eq. (47), which can be achieved for the case in which the total number of proteins inside the cell is very large, i.e., the memory has a large number of possible states. Second, the time scale for changes in states of the fictitious memory must be tuned to some optimal value. For the model system this time scale is characterized by ω_m in Eq. (47). For a system that is more elaborate than our model system one can think of a multi-component memory with the time scale of each component optimally tuned to store information about a certain part of the sensor.

From the chain of inequalities, summarized in Eq. (34), adding the memory raises the learning rate and lowers the upper bound on transfer entropy rate. In a first step, we impose that (i) $C = 1$ and (ii) that the transfer entropy rate is equal to the upper bound, i.e., $l_y = \mathcal{T}_{x \to y} = \overline{\mathcal{T}}_{x \to y}$. From relations (8)

and (18) we obtain

$$\overline{\mathcal{T}}_{x\to y} - l_y = \sum_{y,y'} P(y) \sum_x P(x|y) w_{yy'}^x \ln \frac{P(x|y)w_{yy'}^x}{P(x|y')\overline{w}_{yy'}} \geqslant 0,$$

(61)

where the log sum inequality above is saturated if and only if the term inside the logarithm is independent of x [63]. Hence, if $\overline{\mathcal{T}}_{x\to y} = l_y$ then the rates obey

$$w_{yy'}^x = \frac{P(x|y')}{P(x|y)} \overline{w}_{yy'}.$$

(62)

With this restriction, Eqs. (8) and (20), the entropy production (15) becomes

$$\sigma_y = 2l_y + \tilde{\sigma}_y.$$

(63)

The efficiency (16) then reads

$$\eta_y = \frac{l_y}{\sigma_y} = \frac{1}{2}\frac{\sigma_y - \tilde{\sigma}_y}{\sigma_y} \leqslant \frac{1}{2},$$

(64)

where we used $\sigma_y \geqslant \tilde{\sigma}_y$. Hence, if $C = 1$ and $\mathcal{T}_{x\to y} = \overline{\mathcal{T}}_{x\to y}$, the efficiency fulfills $\eta_y \leqslant 1/2$.

We now demonstrate that $C = 1$ indeed implies $\mathcal{T}_{x\to y} = \overline{\mathcal{T}}_{x\to y}$, which completes the proof of the trade-off. A fictitious memory α is added to the sensor y. The transitions rates are now of the form of Eq. (22) with y replacing r and α replacing m. The learning rate of this fictitious sensor composed of $z = (y,\alpha)$ reads

$$l_z = \sum_{x,x',y,\alpha} P(x,y,\alpha) w^{xx'} \ln \frac{P(x,y,\alpha)}{P(x',y,\alpha)},$$

(65)

where we used Eqs. (10) and (11). Within this fictitious sensor l_y is a coarse-grained learning rate and the difference between l_z and l_y reads

$$l_z - l_y = \sum_{x,x',y} P(x,y) w^{xx'} \sum_\alpha P(\alpha|x,y) \ln \frac{P(\alpha|x,y)}{P(\alpha|x',y)} \geqslant 0.$$

(66)

The assumption $C = 1$ implies $l_y = l_z$. The above inequality is saturated if and only if $P(\alpha|x,y) = P(\alpha|x',y) = P(\alpha|y)$, yielding $P(x|y,\alpha) = \frac{P(y)P(x|y)P(\alpha|x,y)}{P(y)P(\alpha|y)} = P(x|y)$. This relation leads to

$$H[x_t|y_t,\alpha_t] = H[x_t|y_t].$$

(67)

The fictitious memory α is unspecified and the key assumption for our demonstration is that it is always possible for any sensor y to find a fictitious memory α that fulfills the relation

$$H[x_t|y_t,\alpha_t] = H[x_t|\{y_{t'}\}_{t'\leqslant t}].$$

(68)

If we choose such fictitious memory then equality (67) leads to

$$H[x_t|y_t] = H[x_t|\{y_{t'}\}_{t'\leqslant t}].$$

(69)

Hence, if it is possible to find a fictitious memory that fulfills (68), then $C = 1$ implies (69). From (69) we obtain $I[x_t:\{y_{t'}\}_{t'\leqslant t}] = I[x_t:y_t,y_{t-dt}] = I[x_t:y_t]$. The learning rate in

the form (11) can be rewritten as

$$
\begin{aligned}
l_y &= \frac{I[x_t:y_t] - I[x_{t+dt}:y_t]}{dt} \\
&= \frac{I[x_{t+dt}:y_{t+dt}] - I[x_{t+dt}:y_t]}{dt} \\
&= \frac{I[x_{t+dt}:y_{t+dt},y_t] - I[x_{t+dt}:y_t]}{dt},
\end{aligned}
$$

(70)

where we used the steady state property $I[x_{t+dt}:y_{t+dt}] = I[x_t:y_t]$ from the first to the second line. Inserting the conditional probabilities in terms of rates from Eq. (7) into Eq. (70) leads to the completion of the proof, i.e.,

$$l_y = \sum_{x,y,y'} P(x,y) w_{yy'}^x \ln \frac{w_{yy'}^x}{\overline{w}_{yy'}} = \overline{\mathcal{T}}_{x\to y}.$$

(71)

Summarizing, we have demonstrated that $C = 1 \Rightarrow H[x_t|y_t] = H[x_t|\{y_{t'}\}_{t'\leqslant t}] \Rightarrow l_y = \overline{\mathcal{T}}_{x\to y} \Rightarrow C = 1$. This proof also implies that whenever $C = 1$ then the upper bound is also equal to the transfer entropy rate, i.e., $l_y = \mathcal{T}_{x\to y} = \overline{\mathcal{T}}_{x\to y}$. For the coupled linear Langevin equations analyzed in Sec. IV this equality between transfer entropy rate and its upper bound implies the equality between the uncertainty about the external signal that is estimated with the instantaneous state of the sensor and the uncertainty that is estimated with the full time series of the sensor, as shown in Appendix B. For general systems, it remains to be seen whether $C = 1$ implies that both uncertainties are the same.

VI. CONCLUSION

We have introduced the quantity sensory capacity, which provides a measure for the performance of a sensor that follows an external signal. Specifically, the maximal sensory capacity $C = 1$ means that the instantaneous state of the sensor contains the same amount of information about the signal as the full time series of the sensor. As we have shown with the coupled linear Langevin equations in Sec. IV a high sensory capacity can be achieved in two ways. First, for a bare sensor without a memory layer the parameters related to the sensor can be tuned in such a way that $C = 1$. In this case there is no further information available in the full time series of the degree of freedom directly sensing the signal. Second, the more interesting case is when the full time series of this first degree of freedom has more information than its instantaneous state. By adding a memory, which is a second degree of freedom that is influenced by the first degree of freedom but does not react back on it, the sensory capacity can be raised to $C = 1$. This increase in sensory capacity quantifies how much information about the time series of the sensor is stored in the instantaneous state of the memory.

The coupled linear Langevin equations have been derived from a cellular two-component network sensing an external ligand concentration, which is the signal. Within this physical realization of a sensor the first layer of the sensor is the receptors that bind external ligands and the memory is composed of internal proteins that can be phosphorylated. We have shown that the thermodynamic entropy production quantifying dissipation has two terms: work delivered by the external process due to binding and unbinding at different

concentrations and dissipation inside the cell due to ATP hydrolysis. Adding a memory that increases the sensory capacity of a sensor from a low value to a value close to 1 requires a high rate of dissipation inside the cell. Sensory capacity is particularly interesting in this regime of high dissipation, where the efficiency is very low and, therefore, does not characterize well the performance of the sensor.

Finally, we have demonstrated a general trade-off between sensory capacity and efficiency. A sensory capacity $C = 1$ implies an efficiency $\eta \leqslant 1/2$. The limit $\eta = 1/2$ is achieved for a bare sensor with its parameters optimally tuned so that $C = 1$. If these parameters are not optimally tuned, $C = 1$ is possible only with an additional memory that leads to extra dissipation in relation to the bare sensor, which implies $\eta < 1/2$.

This trade-off relation between the two bounded dimensionless quantities C and η provides a further link between information theory and thermodynamics. The sensory capacity C as a ratio between learning rate and transfer entropy rate is of purely information theoretic origin whereas the efficiency η as a ratio between learning rate and entropy production contains input from both fields. As a perspective for future work, the role of nonlinearities in these figures of merit could be explored in more complex models.

An experimental realization verifying the second law for a sensor that involves the rate of dissipated heat and the learning rate is still lacking. A good candidate for such an experiment is a colloidal particle, which is the sensor, subjected to an external potential that is varied stochastically. An experiment with a sensor that has an internal memory seems to be even more challenging.

APPENDIX A: FROM MASTER EQUATION TO LANGEVIN EQUATION IN BIPARTITE PROCESSES

1. Linear noise approximation

We consider a vector $z = (z_1, \ldots, z_d)$ determining the state of the system. Comparing with Sec. II, the first component is related to the signal, i.e., $z_1 = x$. The other components are related to the sensor. If the sensor has only one component r then $z_2 = r$. A sensor with a memory also has a second component $y = (r,m)$, leading to $z_3 = m$. For the variable $z_1 = x$ we denote the transition rate $w^{xx'} = \omega_\pm^{(1)}(z)$ for $x' = x \pm dx$, where dx corresponds to an infinitesimal change in the variable x. The master equation is written as

$$\dot{P}(z) = \sum_{i=1}^{d} [w_+^{(i)}(z - dz_i) P(z - dz_i) - w_+^{(i)}(z) P(z)]$$
$$+ \sum_{i=1}^{d} [w_-^{(i)}(z + dz_i) P(z + dz_i) - w_-^{(i)}(z) P(z)].$$
$$\text{(A1)}$$

With the approximation

$$w_\pm^{(i)}(z \mp dz_i) P(z \mp dz_i) \simeq w_\pm^{(i)}(z) P(z)$$
$$\mp dz_i \frac{\partial}{\partial z_i} w_\pm^{(i)}(z) P(z) + \frac{1}{2} dz_i^2 \frac{\partial^2}{\partial z_i^2} w_\pm^{(i)}(z) P(z), \quad \text{(A2)}$$

the master equation (A1) turns into the Fokker-Planck equation

$$\dot{\rho}(z) = - \sum_i \frac{\partial}{\partial z_i} J_i(z), \quad \text{(A3)}$$

where in the continuous limit $P(z) \to \rho(z) \prod_i dz_i$. The probability current reads

$$J_i(z) \equiv D_i(z) F_i(z) \rho(z) - \frac{\partial}{\partial z_i} D_i(z) \rho(z), \quad \text{(A4)}$$

where

$$D_i(z) F_i(z) \equiv dz_i [w_+^{(i)}(z) - w_-^{(i)}(z)] \quad \text{(A5)}$$

and

$$D_i(z) \equiv \frac{dz_i^2}{2} [w_+^{(i)}(z) + w_-^{(i)}(z)]. \quad \text{(A6)}$$

Within the Ito interpretation [66,67], the Fokker-Planck equation (A3) corresponds to the Langevin equation

$$\dot{z}_{i,t} = D_i(z_t) F_i(z_t) + \xi_t^i, \quad \text{(A7)}$$

where $\langle \xi_t^i \xi_{t'}^j \rangle = 2 D_i(z) \delta_{ij} \delta(t - t')$. The δ_{ij} term in this last equation is a direct consequence of the bipartite (or multipartite) structure of the transition rates.

2. Two-component network with a weakly fluctuating signal

The linear noise approximation for the specific model of Sec. III is valid in the limit $N_y, N_b \gg 1$ and $dx \to 0$. In this case, from the transition rates (35), (38), and (42), the Langevin equation (A7) becomes

$$\dot{x}_t = -\omega_x x_t + \xi_t^x,$$
$$\dot{n}_b(t) = \omega_r^+(x_t) N_b - [\omega_r^+(x_t) + \omega_r^-(x_t)] n_b(t) + \xi_t^b,$$
$$\dot{n}_y(t) = \omega_y^+(n_b(t)) N_y - [\omega_m^+(n_b(t)) + \omega_m^-(n_b(t))] n_y(t) + \xi_t^y.$$
$$\text{(A8)}$$

From Eq. (A6), the noise terms ξ_t^b and ξ_t^y fulfill a relation similar to (37), with amplitudes

$$D_b(x, n_b) = \tfrac{1}{2} [\omega_r^+(x)(N_b - n_b) + \omega_r^-(x) n_b],$$
$$D_y(n_b, n_y) = \tfrac{1}{2} [\omega_m^+(n_b)(N_y - n_y) + \omega_m^-(n_b) n_y], \quad \text{(A9)}$$

respectively.

If the fluctuations of the signal are small such that x stays close to the value $x = 0$ we can apply the following expansion:

$$N_b \omega_r^+(x) / [\omega_r^+(x) + \omega_r^-(x)] \equiv n_b^* + \alpha_1 x + O(x)^2, \quad \text{(A10)}$$

where $n_b^* \equiv N_b \omega_r^+(0) / [\omega_r^+(0) + \omega_r^-(0)]$ and α_1 is the first derivative evaluated at $x = 0$. For $n_b - n_b^*$ small,

$$N_y \omega_m^+(n_b) / [\omega_m^+(n_b) + \omega_m^-(n_b)]$$
$$\equiv n_y^* + \alpha_2 (n_b - n_b^*) + O(n_b - n_b^*)^2, \quad \text{(A11)}$$

where $n_y^* \equiv N_y \omega_m^+(n_b^*) / [\omega_m^+(n_b^*) + \omega_m^-(n_b^*)]$ and α_2 is the first derivative evaluated at $n_b = n_b^*$. In the limit where Eqs. (A10) and (A11) are valid, the Langevin equations (A8)

become

$$\dot{x}_t = -\omega_x x_t + \xi_t^x,$$

$$\dot{n}_b(t) = \omega_r[n_b^* + \alpha_1 x_t - n_b(t)] + \xi_t^b, \qquad \text{(A12)}$$

$$\dot{n}_y(t) = \omega_m[n_y^* + \alpha_2[n_b(t) - n_b^*] - n_y(t)] + \xi_t^y,$$

where

$$\omega_r \equiv \omega_r^+(0) + \omega_r^-(0),$$

$$\omega_m \equiv \omega_m^+(n_b^*) + \omega_m^-(n_b^*). \qquad \text{(A13)}$$

Furthermore, the noise amplitudes in Eq. (A9) become

$$D_b^* \equiv D_b(0,n_b^*) = \frac{\omega_r}{N_b} n_b^*(N_b - n_b^*),$$

$$D_y^* \equiv D_y(n_b^*,n_y^*) = \frac{\omega_m}{N_y} n_y^*(N_y - n_y^*). \qquad \text{(A14)}$$

The explicit form of the parameter α_1 in Eq. (A10) is

$$\alpha_1 = \frac{n_b^*(N_b - n_b^*)}{N_b} \frac{\partial \Delta F(x)}{\partial x} \qquad \text{(A15)}$$

and α_2 in Eq. (A11) is

$$\alpha_2 = \frac{n_y^*(N_y - n_y^*)}{N_y}\left[\frac{\kappa_+ \nu_+ - \kappa_- \nu_-}{(n_b^*\kappa_+ + \nu_-)(n_b^*\kappa_- + \nu_+)}\right], \qquad \text{(A16)}$$

as obtained from (41). Hence, for $\Delta\mu = \ln[\kappa_+\nu_+/(\kappa_-\nu_-)] = 0$ this last parameter is $\alpha_2 = 0$; i.e., the memory level in Eq. (A12) is not affected by the number of occupied receptors. Therefore, ATP consumption is necessary in order for the memory to be able to store information about the signal.

The linear Langevin equations can be further simplified with the transformations

$$r_t \equiv \frac{n_b(t) - n_b^*}{\alpha_1} \qquad \text{(A17)}$$

and

$$m_t \equiv \frac{n_y(t) - n_y^*}{\alpha_1\alpha_2}. \qquad \text{(A18)}$$

With these variables the Langevin equations (A12) become Eq. (47), with the noise amplitudes (A14) transformed to

$$D_r = D_b^*/\alpha_1^2,$$

$$D_m = D_y^*/(\alpha_1\alpha_2)^2. \qquad \text{(A19)}$$

From Eqs. (A14)–(A16) we obtain

$$D_r = \frac{\omega_r N_b}{n_b^*(N_b - n_b^*)}\left[\frac{\partial \Delta F(x)}{\partial x}\right]^{-2},$$

$$D_m = \left[\frac{N_b}{n_b^*(N_b - n_b^*)}\right]^2 \left[\frac{\partial \Delta F(x)}{\partial x}\right]^{-2} \qquad \text{(A20)}$$

$$\times \frac{\omega_m N_y}{n_y^*(N_y - n_y^*)}\left[\frac{(n_b^*\kappa_+ + \nu_-)(n_b^*\kappa_- + \nu_+)}{\kappa_+\nu_+ - \kappa_-\nu_-}\right]^2,$$

where according to (A10) $n_b^* \sim N_b$ and according to (A11) $n_y^* \sim N_y$. Hence, $D_r \sim N_b^{-1}$; i.e., the noise amplitude related to the receptor decreases with increasing total number of receptors N_b. Moreover, the memory noise D_m is inversely

proportional to the total number of internal proteins N_y and diverges for $\Delta\mu \equiv \ln[\kappa_+\nu_+/(\kappa_-\nu_-)] \to 0$.

3. Quantities in the continuum limit

We consider a vector $(z_1,z_2,z_3) = (x,r,m)$ with transition rates

$$\omega_\pm^{(1)}(z) \equiv \frac{D_x}{dx^2}\exp\left[\pm\frac{F_x(x)dx}{2}\right], \qquad \text{(A21)}$$

$$\omega_\pm^{(2)}(z) \equiv \frac{D_r}{dr^2}\exp\left[\pm\frac{F_r(x,r)dr}{2}\right], \qquad \text{(A22)}$$

$$\omega_\pm^{(3)}(z) \equiv \frac{D_m}{dm^2}\exp\left[\pm\frac{F_m(r,m)dm}{2}\right], \qquad \text{(A23)}$$

where the diffusion constants D_i are assumed to be independent of (x,r,m). The following relations are obtained by taking their expressions for the discrete case in Sec. II and then taking the continuous limit $(dx,dr,dm) \to 0$, where the probability is replaced by a density, i.e., $P(x,r,m) \to \rho(x,r,m)dx\,dr\,dm$.

Learning rate. From Eqs. (A2) and (A4) the learning rate (8) becomes

$$l_y = \int dx \int dr \int dm\, J_r(x,r,m)\frac{\partial}{\partial r}\ln\rho(x|r,m)$$

$$+ \int dx \int dr \int dm\, J_m(x,r,m)\frac{\partial}{\partial m}\ln\rho(x|r,m), \qquad \text{(A24)}$$

where $\rho(x|r,m) \equiv \rho(x,r,m)/[\int \rho(\tilde{x},r,m)d\tilde{x}]$. This expression can also be found in Ref. [46], where the learning rate is called information flow. Integration by parts and the steady state property $\partial_x J_x + \partial_r J_r + \partial_m J_m = 0$ leads to the alternative expression

$$l_y = -\int dx \int dr \int dm\, J_x(s,r,m)\frac{\partial}{\partial x}\ln\rho(x|r,m). \qquad \text{(A25)}$$

Coarse-grained learning rate. The coarse-grained learning rate in Eq. (23) becomes

$$l_r = -\int dx \int dr\, J_r(x,r)\frac{\partial}{\partial r}\ln\rho(x|r), \qquad \text{(A26)}$$

where $J_r(x,r) \equiv \int dm\, J_r(x,r,m)$, $\rho(x,r) \equiv \int dm\rho(x,r,m)$, and $\rho(x|r) \equiv \rho(x,r)/[\int \rho(\tilde{x},r)d\tilde{x}]$.

Entropy production. The entropy production in Eq. (15) is separated into two contributions

$$\sigma_y \equiv \sigma_r + \sigma_m, \qquad \text{(A27)}$$

as shown in Eqs. (43) and (45). In the continuous limit, using Eqs (A2) and (A4), these contributions become

$$\sigma_r = \int dx \int dr \int dm\, J_r(x,r)F_r(x,r) \qquad \text{(A28)}$$

and

$$\sigma_m = \int dx \int dr \int dm\, J_m(x,r,m)F_m(r,m). \qquad \text{(A29)}$$

Coarse-grained entropy production. From Eqs. (A2), (A4), and (A29), the coarse-grained entropy production (20)

becomes

$$\tilde{\sigma}_{y} = \int dr \int dm \left[\int J_r(x,r,m)dx \right] \left[\int F_r(\tilde{x},r)\rho(\tilde{x}|r,m)d\tilde{x} \right] + \sigma_m.$$

(A30)

The last term σ_m remains the same because m is not directly influenced by the signal x.

Upper bound on transfer entropy rate. The upper bound of the transfer entropy rate (18) becomes

$$\overline{\mathcal{T}}_{x \to y} = \frac{D_r}{4} \int dx \int dr \int dm \rho(x,r,m)[F_r(x,r)^2 - \tilde{F}_r(r,m)^2],$$

(A31)

where we used the averaged force

$$\tilde{F}_r(r,m) \equiv \int dx \rho(x|r,m)F_r(x,r).$$

(A32)

Since $\tilde{F}_m(r,m) = F_m(r,m)$, the contribution due to m is zero. For $\overline{\mathcal{T}}_{x \to r}$ defined in Eq. (33) we replace $\rho(x|r,m)$ by $\rho(x|r)$ in Eqs. (A32) and (A31), which leads to the expression

$$\overline{\mathcal{T}}_{x \to r} = \frac{D_r}{4} \int dx \int dr \rho(x,r)[F_r(x,r)^2 - \tilde{F}_r(r)^2],$$

(A33)

where $\tilde{F}_r(r) \equiv \int dx \rho(x|r)F_r(x,r)$.

4. Gaussian linear processes

We now consider a linear Langevin equation of the form

$$\begin{pmatrix} \dot{x}_t \\ \dot{y}_t \end{pmatrix} = -\mathbf{A} \begin{pmatrix} x_t \\ y_t \end{pmatrix} + \boldsymbol{\xi}_t,$$

(A34)

where $\langle \boldsymbol{\xi}_t \boldsymbol{\xi}_{t'}^{\top} \rangle = 2\mathbf{D}\delta(t - t')$. The matrices $\mathbf{A}$ and $\mathbf{D}$ for the bare sensor $y = r$ are given by (50) and for the sensor with a memory $y = (r,m)$ they are given by (56). The steady state solution of this Langevin equation is a multivariate normal distribution $\rho(x,y)$ with zero mean and covariance $\boldsymbol{\Sigma}$, which is the stationary solution of (49). Comparing Eqs. (A7) and (A34) the drift term is

$$\boldsymbol{F}(x,y) \equiv -\mathbf{D}^{-1}\mathbf{A} \begin{pmatrix} x \\ y \end{pmatrix}.$$

(A35)

The probability current defined in Eq. (A4) is then given by

$$\boldsymbol{J}(x,y) = -[\mathbf{A} - \mathbf{D}\boldsymbol{\Sigma}^{-1}] \begin{pmatrix} x \\ y \end{pmatrix} \rho(x,y),$$

(A36)

where $\boldsymbol{\Sigma}^{-1}$ is the inverse of $\boldsymbol{\Sigma}$.

We define the matrix

$$\boldsymbol{\Phi} \equiv \int dx \int dy \, \boldsymbol{J}(x,y)\boldsymbol{F}(x,y)^{\top}.$$

(A37)

Equations (A35) and (A36) yield

$$\boldsymbol{\Phi} = [\mathbf{A} - \mathbf{D}\boldsymbol{\Sigma}^{-1}]\boldsymbol{\Sigma}\mathbf{A}^{\top}\mathbf{D}^{-1} = \mathbf{A}\boldsymbol{\Sigma}\mathbf{A}^{\top}\mathbf{D}^{-1} - \mathbf{D}\mathbf{A}^{\top}\mathbf{D}^{-1},$$

(A38)

where we used the fact that $\rho(x,y)$ is a multivariate Gaussian density. With this expression, from Eq. (A28) we obtain

$$\sigma_r = \Phi_{rr} = \omega_x \frac{\nu_r^2}{B_r(1 + \nu_r)},$$

(A39)

and from Eq. (A29) we obtain

$$\sigma_m = \Phi_{mm} = \omega_x \frac{\nu_m^2 [\nu_r^2 + B_r(1 + \nu_m)(1 + \nu_r)]}{B_m(1 + \nu_m)(1 + \nu_r)(\nu_m + \nu_r)},$$

(A40)

where $\mathcal{E}_x^2 \equiv D_x/\omega_x, \nu_r \equiv \omega_r/\omega_x, B_r \equiv D_r/D_x, \nu_m \equiv \omega_m/\omega_x, B_m \equiv D_m/D_x$ (as defined in Sec. IV).

The gradient of the log of the density reads

$$\boldsymbol{a}(x,y) \equiv -\begin{pmatrix} \partial_x \\ \partial_y \end{pmatrix} \ln \rho(x,y) = \boldsymbol{\Sigma}^{-1} \begin{pmatrix} x \\ y \end{pmatrix}.$$

(A41)

With the matrix

$$\mathbf{L} \equiv \int dx \int dy \, \boldsymbol{J}(x,y)\boldsymbol{a}(x,y)^{\top}$$

$$= -(\mathbf{A} - \mathbf{D}\boldsymbol{\Sigma}^{-1})\boldsymbol{\Sigma}\boldsymbol{\Sigma}^{-1} = -\mathbf{A} + \mathbf{D}\boldsymbol{\Sigma}^{-1},$$

(A42)

where we used Eqs. (A36) and (A41), the learning rate $l_y = \mathbf{L}_{xx}$ (A25) reads

$$l_y = \mathbf{L}_{xx} = \omega_x [-1 + \mathcal{E}_x^2 (\boldsymbol{\Sigma}^{-1})_{xx}].$$

(A43)

The 2×2 covariance matrix of (x,r) given by (51) yields

$$l_r = \mathbf{L}_{xx} = \omega_x \frac{\nu_r^3}{\nu_r^2 + B_r(1 + \nu_r)^2}.$$

(A44)

For a the case with memory, where $(x,y) = (x,r,m)$, the explicit form of the learning rate (A43) is given by

$$l_y = \mathbf{L}_{xx}$$

$$= \frac{\omega_x \nu_r^2 (\nu_m + \nu_r)\{B_r \nu_m^2 (\nu_m \nu_r + 1) + \nu_r [B_m(\nu_m + 1)^2(\nu_m + \nu_r) + \nu_m^2 \nu_r]\}}{\nu_m^2 \{B_r \nu_r^2 [\nu_m^2 + \nu_m(4\nu_r + 2) + \nu_r^2 + 2\nu_r + 2] + B_r^2(\nu_m + 1)^2(\nu_r + 1)^2 + \nu_r^4\} + B_m(\nu_m + 1)^2 [B_r(\nu_r + 1)^2 + \nu_r^2](\nu_m + \nu_r)^2}.$$

(A45)

The upper bound on the transfer entropy rate (A31) reads

$$\overline{\mathcal{T}}_{x \to y} = \frac{\omega_r^2}{4D_r} \int dx \int dr \int dm \, \rho(x,r,m)[x^2 - \langle x|r,m \rangle^2],$$

(A46)

where $\langle x|r,m \rangle \equiv \int \rho(\tilde{x}|r,m)\tilde{x} \, d\tilde{x}$ and we used $F_r(x,r) = \omega_r(x - r)/D_r$.

APPENDIX B: UNCERTAINTY FROM INSTANTANEOUS STATE AND FROM TIME SERIES

We first consider a sensor with memory $y = (r,m)$. The covariance matrix, which is the stationary solution of (49) with matrices given by (56), is written as

$$\mathbf{\Sigma} = \begin{pmatrix} \Sigma_{xx} & \Sigma_{xr} & \Sigma_{xm} \\ \Sigma_{xr} & \Sigma_{rr} & \Sigma_{rm} \\ \Sigma_{xm} & \Sigma_{rm} & \Sigma_{mm} \end{pmatrix} \equiv \begin{pmatrix} \mathcal{E}_x^2 & \boldsymbol{b}^\top \\ \boldsymbol{b} & \tilde{\mathbf{\Sigma}} \end{pmatrix}. \quad \text{(B1)}$$

The linear estimate of x from $\boldsymbol{y}$ is $\hat{x}(\boldsymbol{y}) \equiv \boldsymbol{c}^\top \boldsymbol{y}$, where $\mathbf{c}$ is a vector. Minimizing the variance

$$\langle [x - \hat{x}(\boldsymbol{y})]^2 \rangle = \mathcal{E}_x^2 - 2\boldsymbol{c}^\top \boldsymbol{b} + \boldsymbol{c}^\top \tilde{\mathbf{\Sigma}} \boldsymbol{c}, \quad \text{(B2)}$$

which is minimal for $\boldsymbol{c} = \tilde{\mathbf{\Sigma}}^{-1}\boldsymbol{b}$, leads to the uncertainty

$$\mathcal{E}_{x|y}^2 = \mathcal{E}_x^2 - \boldsymbol{b}^\top \tilde{\mathbf{\Sigma}}^{-1}\boldsymbol{b} = \mathcal{E}_x^2 \left(1 - \frac{\boldsymbol{b}^\top \tilde{\mathbf{\Sigma}}^{-1}\boldsymbol{b}}{\mathcal{E}_x^2}\right). \quad \text{(B3)}$$

Following the same procedure for a bare sensor with $\boldsymbol{y} = r$, $\tilde{\mathbf{\Sigma}} = \Sigma_{rr}$, and $\boldsymbol{b} = \Sigma_{xr} = \boldsymbol{b}^\top$, the covariance matrix (51) leads to an uncertainty

$$\mathcal{E}_{x|r}^2 = \mathcal{E}_x^2 \left[1 - \frac{\nu_r^3}{\nu_r^3 + \nu_r^2 + B_r(1 + \nu_r)^2}\right]. \quad \text{(B4)}$$

Comparing Eq. (55) with Eq. (B4) we obtain

$$\overline{\mathcal{T}}_{x\to r} = \frac{\omega_x \nu_r^2}{4B_r} \frac{\mathcal{E}_{x|r}^2}{\mathcal{E}_x^2}. \quad \text{(B5)}$$

Likewise, from Eq. (A46), with $\rho(x,r,m)$ a multivariate Gaussian with zero mean and covariance matrix (B1), and

Eq. (B3) we obtain

$$\overline{\mathcal{T}}_{x\to y} = \frac{\omega_x \nu_r^2}{4B_r} \frac{\mathcal{E}_{x|y}^2}{\mathcal{E}_x^2}. \quad \text{(B6)}$$

The best estimate $\hat{x}_t$ that uses the time series of the sensor $\{r_{t'}\}_{t' \leqslant t}$ to minimize the uncertainty $\hat{\mathcal{E}}_t^2 \equiv \langle (x_t - \hat{x}_t)^2 \rangle$ is known as the Kalman-Bucy filter [45,68]. For the linear Gaussian process from (47) the best estimate $\hat{x}_t$ satisfies $\langle r_{t'}\hat{x}_t \rangle = \langle r_{t'}x_t \rangle$ for all $t' \leqslant t$ and $\langle \hat{x}_t(x_t - \hat{x}_t) \rangle = 0$ (see [68]). It can be shown that the minimal error satisfies the Riccati equation, which reads [45,68]

$$\frac{d}{dt}\hat{\mathcal{E}}_t^2 = -\frac{\omega_r^2}{2D_r}\hat{\mathcal{E}}_t^4 - 2\omega_x\hat{\mathcal{E}}_t^2 + 2D_x. \quad \text{(B7)}$$

The stationary solution of this equation gives the uncertainty about the signal given the sensor trajectory

$$\mathcal{E}_{x|r_{\text{traj}}}^2 = \mathcal{E}_x^2 \left(\frac{2}{1 + \sqrt{1 + \frac{\nu_r^2}{B_r}}}\right). \quad \text{(B8)}$$

Comparing with Eq. (53) we obtain

$$\mathcal{T}_{x\to r} = \frac{\omega_x \nu_r^2}{4B_r} \frac{\mathcal{E}_{x|r_{\text{traj}}}^2}{\mathcal{E}_x^2}. \quad \text{(B9)}$$

The simple relations (B5), (B6), and (B9) are valid for our model system that corresponds to a linear Gaussian process. Since for $C = 1$ the transfer entropy rate equals its upper bound, for our model system a maximal sensory capacity $C = 1$ implies $\mathcal{E}_{x|r_{\text{traj}}} = \mathcal{E}_{x|y}$. In this case the linear estimate $\hat{x}(\boldsymbol{y}) = \boldsymbol{c}^\top \boldsymbol{y} = \boldsymbol{b}^\top \tilde{\mathbf{\Sigma}}^{-1}\boldsymbol{y}$ from Eq. (B2) coincides with the estimate from the Kalman-Bucy filter $\hat{x}_t$, which is similar to the finding in Ref. [45] for optimal feedback cooling.

---

[1] J. M. R. Parrondo, J. M. Horowitz, and T. Sagawa, Nat. Phys. **11**, 131 (2015).

[2] A. Berut, A. Arakelyan, A. Petrosyan, S. Ciliberto, R. Dillenschneider, and E. Lutz, Nature (London) **483**, 187 (2012).

[3] Y. Jun, M. Gavrilov, and J. Bechhoefer, Phys. Rev. Lett. **113**, 190601 (2014).

[4] S. Toyabe, T. Sagawa, M. Ueda, E. Muneyuki, and M. Sano, Nat. Phys. **6**, 988 (2010).

[5] J. V. Koski, V. F. Maisi, T. Sagawa, and J. P. Pekola, Phys. Rev. Lett. **113**, 030601 (2014).

[6] E. Roldán, I. A. Martínez, J. M. R. Parrondo, and D. Petrov, Nat. Phys. **10**, 457 (2014).

[7] T. Sagawa and M. Ueda, Phys. Rev. Lett. **100**, 080403 (2008).

[8] F. J. Cao and M. Feito, Phys. Rev. E **79**, 041118 (2009).

[9] T. Sagawa and M. Ueda, Phys. Rev. Lett. **104**, 090602 (2010).

[10] J. M. Horowitz and S. Vaikuntanathan, Phys. Rev. E **82**, 061120 (2010).

[11] J. M. Horowitz and J. M. R. Parrondo, EPL **95**, 10005 (2011).

[12] L. Granger and H. Kantz, Phys. Rev. E **84**, 061110 (2011).

[13] D. Abreu and U. Seifert, EPL **94**, 10001 (2011).

[14] D. Abreu and U. Seifert, Phys. Rev. Lett. **108**, 030601 (2012).

[15] M. Bauer, D. Abreu, and U. Seifert, J. Phys. A: Math. Theor. **45**, 162001 (2012).

[16] T. Munakata and M. L. Rosinberg, J. Stat. Mech. (2012) P05010.

[17] T. Munakata and M. L. Rosinberg, J. Stat. Mech. (2013) P06014.

[18] T. Sagawa and M. Ueda, Phys. Rev. E **85**, 021104 (2012).

[19] S. Ito and T. Sagawa, Phys. Rev. Lett. **111**, 180603 (2013).

[20] J. M. Horowitz, T. Sagawa, and J. M. R. Parrondo, Phys. Rev. Lett. **111**, 010602 (2013).

[21] P. Strasberg, G. Schaller, T. Brandes, and M. Esposito, Phys. Rev. Lett. **110**, 040601 (2013).

[22] M. Bauer, A. C. Barato, and U. Seifert, J. Stat. Mech. (2014) P09010.

[23] H. Sandberg, J.-C. Delvenne, N. J. Newton, and S. K. Mitter, Phys. Rev. E **90**, 042119 (2014).

[24] M. Prokopenko and J. T. Lizier, Sci. Rep. **4**, 5394 (2014).

[25] M. Prokopenko and I. Einav, Phys. Rev. E **91**, 062143 (2015).

[26] M. L. Rosinberg, T. Munakata, and G. Tarjus, Phys. Rev. E **91**, 042114 (2015).

[27] J. Bechhoefer, New J. Phys. **17**, 075003 (2015).

[28] N. Shiraishi and T. Sagawa, Phys. Rev. E **91**, 012130 (2015).

[29] N. Shiraishi, S. Ito, K. Kawaguchi, and T. Sagawa, New J. Phys. **17**, 045012 (2015).

[30] D. Mandal and C. Jarzynski, Proc. Natl. Acad. Sci. USA **109**, 11641 (2012).

[31] D. Mandal, H. T. Quan, and C. Jarzynski, Phys. Rev. Lett. **111**, 030602 (2013).

[32] S. Deffner and C. Jarzynski, Phys. Rev. X **3**, 041003 (2013).

[33] S. Deffner, Phys. Rev. E **88**, 062128 (2013).

[34] A. C. Barato and U. Seifert, EPL **101**, 60001 (2013).

[35] A. C. Barato and U. Seifert, Phys. Rev. Lett. **112**, 090601 (2014).

[36] A. C. Barato and U. Seifert, Phys. Rev. E **90**, 042150 (2014).

[37] J. Hoppenau and A. Engel, EPL **105**, 50002 (2014).

[38] N. Merhav, J. Stat. Mech. (2015) P06037.

[39] A. B. Boyd, D. Mandal, and J. P. Crutchfield, arXiv:1507.01537.

[40] A. E. Allahverdyan, D. Janzing, and G. Mahler, J. Stat. Mech. (2009) P09011.

[41] A. C. Barato, D. Hartich, and U. Seifert, J. Stat. Phys. **153**, 460 (2013).

[42] D. Hartich, A. C. Barato, and U. Seifert, J. Stat. Mech. (2014) P02016.

[43] G. Diana and M. Esposito, J. Stat. Mech. (2014) P04010.

[44] J. M. Horowitz and M. Esposito, Phys. Rev. X **4**, 031015 (2014).

[45] J. M. Horowitz and H. Sandberg, New J. Phys. **16**, 125007 (2014).

[46] J. M. Horowitz, J. Stat. Mech. (2015) P03006.

[47] G. Lan, P. Sartori, S. Neumann, V. Sourjik, and Y. Tu, Nat. Phys. **8**, 422 (2012).

[48] P. Mehta and D. J. Schwab, Proc. Natl. Acad. Sci. USA **109**, 17978 (2012).

[49] A. C. Barato, D. Hartich, and U. Seifert, Phys. Rev. E **87**, 042104 (2013).

[50] G. De Palo and R. G. Endres, PLoS Comput. Biol. **9**, e1003300 (2013).

[51] M. Skoge, S. Naqvi, Y. Meir, and N. S. Wingreen, Phys. Rev. Lett. **110**, 248102 (2013).

[52] A. H. Lang, C. K. Fisher, T. Mora, and P. Mehta, Phys. Rev. Lett. **113**, 148103 (2014).

[53] C. C. Govern and P. R. ten Wolde, Phys. Rev. Lett. **113**, 258102 (2014).

[54] C. C. Govern and P. R. ten Wolde, Proc. Natl. Acad. Sci. USA **111**, 17486 (2014).

[55] A. C. Barato, D. Hartich, and U. Seifert, New J. Phys. **16**, 103024 (2014).

[56] P. Sartori, L. Granger, C. F. Lee, and J. M. Horowitz, PLoS Comput. Biol. **10**, e1003974 (2014).

[57] D. Hartich, A. C. Barato, and U. Seifert, New J. Phys. **17**, 055026 (2015).

[58] S. Bo, M. Del Giudice, and A. Celani, J. Stat. Mech. (2015) P01014.

[59] S. Ito and T. Sagawa, Nat. Commun. **6**, 7498 (2015).

[60] S. Still, D. A. Sivak, A. J. Bell, and G. E. Crooks, Phys. Rev. Lett. **109**, 120604 (2012).

[61] G. Aquino, L. Tweedy, D. Heinrich, and R. G. Endres, Sci. Rep. **4**, 5688 (2014).

[62] T. Schreiber, Phys. Rev. Lett. **85**, 461 (2000).

[63] T. M. Cover and J. A. Thomas, *Elements of Information Theory*, 2nd ed. (Wiley-Interscience, Hoboken, NJ, 2006).

[64] U. Seifert, Rep. Prog. Phys. **75**, 126001 (2012).

[65] M. Esposito, Phys. Rev. E **85**, 041125 (2012).

[66] C. W. Gardiner, *Handbook of Stochastic Methods*, 3rd ed. (Springer, Berlin, 2004).

[67] P. C. Bressloff, *Stochastic Processes in Cell Biology* (Springer International Publishing, Cham, 2014).

[68] B. Øksendal, *Stochastic Differential Equations* (Springer, Berlin, 2003).